Environmental Science & Technology Letters

pubs.acs.org/journal/estlcu

Letter

Atmospheric Processing of Particulate Imidazole Compounds Driven by Photochemistry

Xiaodong Hu, Ziyong Guo, Wei Sun, Xiufeng Lian, Yuzhen Fu, He Meng, Yujiao Zhu, Guohua Zhang,* Xinfeng Wang, Likun Xue, Xinhui Bi, Xinming Wang, and Ping'an Peng

Cite This: *Environ. Sci. Technol. Lett.* 2022, 9, 265−271

Read Online

ACCESS | Metrics & More | Article Recommendations | Supporting Information

ABSTRACT: As a potential fraction of brown carbon, particulate imidazole compounds may initiate photosensitive reactions and have substantial radiative effects. However, our knowledge of the atmospheric processing of imidazole compounds is still in its nascent stage. On the basis of a single-particle aerosol mass spectrometer measurement, the mixing state of imidazole-containing particles and high-time-resolved variations of imidazole compounds were investigated in Qingdao, China, in November and December 2019. Five imidazole compounds (methylimidazole, ethylimidazole, dimethylimidazole, imidazole-2-carboxaldehyde, and 2,2′-biimidazole) were identified, overall accounting for ∼10% of all of the detected particles. They are tightly correlated and internally mixed with enhanced carbonyls, amines, and ammonium, supporting their secondary formation from these precursors. The number fraction of imidazole-containing particles exhibited predominant diurnal variations, especially on sunny days. A sharp decrease in the number fraction from morning to noon is most likely attributed to photochemical degradation. This is also confirmed by the reverse correlation ($r = -0.77$; $p < 0.01$) with photochemical indicators (temperature and O_3) and our laboratory experiment by exposure of imidazole compounds to sunlight. Multiple linear regression and random forest analysis further support the hypothesis, with precursors (i.e., carbonyls and amines/ammonium) and O_3 being the most important factors (∼70%) regulating the variations of imidazole compounds.

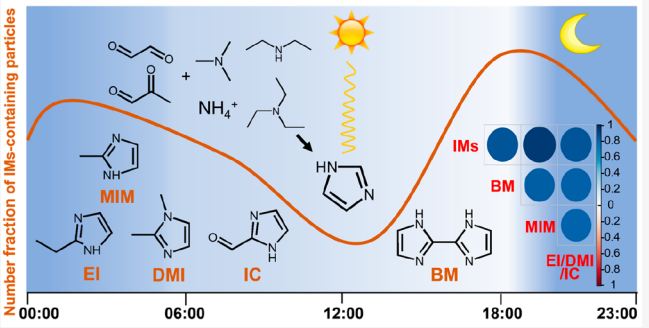

KEYWORDS: *imidazole compounds, individual particles, carbonyls, SPAMS, brown carbon*

INTRODUCTION

As a substantial part of brown carbon, imidazole compounds (IMs) show strong light-absorbing properties and thus affect the atmospheric radiation balance.[1,2] Some fractions could act as photosensitizers, such as imidazole-2-carboxaldehyde (IC) and 2,2′-biimidazole (BM), and may be potential photosensitizers for other aerosol-phase reactions.[3,4] They also contribute to the formation of high-molecular-weight compounds by acting as reaction intermediates.[5−8] In addition, some of them are possibly carcinogenic to humans; e.g., 2-methylimidazole and 4-methylimidazole are categorized as group 2B carcinogens by the International Agency for Research on Cancer (IARC),[9] yet the potential health effects of IMs in atmospheric aerosols remain unknown.

Particulate IMs could be emitted from biomass burning and secondarily formed in the atmosphere.[9−11] A growing body of evidence from laboratory studies has indicated the formation of IMs from the aqueous-phase or heterogeneous reactions of carbonyl compounds and reduced nitrogen species (e.g., ammonium/amines).[3−5,12−20] These kinds of reactions produce various IMs, including methylimidazole (MIM) and dimethylimidazole (DMI), 1,3,4-trimethylimidazole, 4-methyl-1,3-diglycine-imidazole, IC, BM, etc. The secondary formation of IMs could be affected by the abundance and types of precursors (i.e., carbonyls and reduced nitrogen species),[21,22] relative humidity (RH),[23] and pH.[7]

The sinks of atmospheric IMs are most likely associated with reactive oxidants and direct photochemistry. Theoretical calculations and laboratory reaction kinetic studies show that IMs can be rapidly oxidized and degraded by OH radicals, with an atmospheric lifetime over a wide range from 1 min to 1.8 days.[24] Some studies have also shown the oxidation of IMs by ozone (O_3), but the reaction rate is 4 orders of magnitude lower than that by OH radicals.[25,26] In addition, direct photolysis may also contribute.[27]

While extensive laboratory studies have investigated the formation and evolution of various IMs and influencing factors,

Received: January 12, 2022
Revised: March 18, 2022
Accepted: March 18, 2022
Published: March 23, 2022

https://doi.org/10.1021/acs.estlett.2c00029
Environ. Sci. Technol. Lett. 2022, 9, 265−271

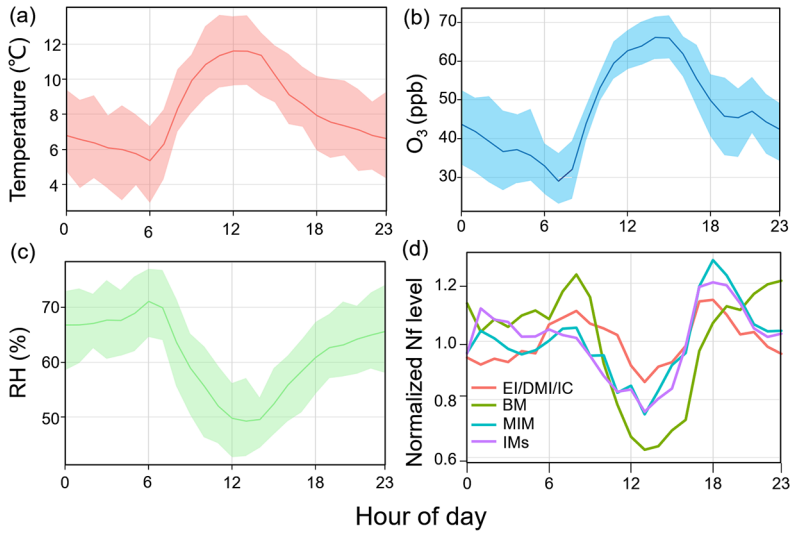

Figure 1. Diurnal variations of (a) temperature, (b) O_3, and (c) relative humidity (RH) during the measurements. The lines and the shaded areas represent the mean and 10−90th percentile values, respectively. (d) Normalized (divided by their mean values) diurnal variations of the Nf of the IMs-containing particles.

the atmospheric processing of these compounds is still in a nascent stage. A few studies have investigated particulate IMs (PM_1, PM_{10}, and TSP) in the atmosphere in China, Germany, Italy, and Japan, most of which focused on their concentrations. The reported concentrations were in the range of 0.01−20.99 ng m^{-3}; the most abundant was 4(5)-methylimidazole, followed by 2-ethylimidazole (EI), DMI, and IC.[1,2,9,11,28] Teich et al.[9] observed higher concentrations of IMs at night than during the day and attributed these observations to the photochemical process and boundary layer height. He et al.[28] showed that RH and salting effect may have an influence on the formation of secondary IMs. Recently, using a single-particle aerosol mass spectrometer (SPAMS), we first provided direct evidence for the formation of IMs from carbonyls and ammonium/amines in the ambient atmosphere and showed the facilitated formation of IMs under cloud conditions.[29] However, most of the field observations employed offline analysis with poor temporal resolution, which may inhibit our in-depth understanding of the ever-changing nature of light-sensitive IMs.

In this study, the chemical compositions of individual IMs-containing particles were investigated by the SPAMS with a high time resolution over a month in a coastal city in northern China. We first identify different kinds of IMs and illustrate their state of mixing with various species. Then we focus on the diurnal variations of IMs and aim to illustrate the controlling factors for the atmospheric processing of IMs.

MATERIALS AND METHODS

Field Measurements. Field measurements were taken at Qingdao Blue Valley Venture Center (36.35°N, 120.68°E), with the sampling inlet on the top of a four-floor building, from November 7 to December 5, 2019. The site is surrounded by villages, close to a highway, and 40 km from downtown Qingdao, representative of a typical suburban environment.[30] During the measurements, the diurnal variations of temperature, RH, and O_3 were distinct, as shown in Figure 1. Temperature and O_3 peaked at noon, whereas RH peaked at night. The temporal variations of meteorological parameters and concentrations of various pollutants (with the instruments described in Text S1), including O_3, NO_2, SO_2, and black carbon (BC), are also included in Figure S1. The average temperature (mean ± standard deviation) is 8.0 ± 6.1 °C, and the average concentrations of $PM_{2.5}$ and PM_{10} are 40.1 ± 21.2 and 69.9 ± 38.9 $\mu g\ m^{-3}$, respectively. The average concentrations of NO_2 and O_3 are 24.8 ± 15.2 and 47.3 ± 23.6 ppbv, respectively.

The size and chemical composition of individual aerosol particles were obtained by the SPAMS (Hexin Analytical Instrument Co., Ltd., Guangzhou, China) in real time. Briefly, the aerosol particles were introduced into the SPAMS by a $PM_{2.5}$ inlet followed by a silica gel dryer. The aerosol particles passed through an aerodynamic lens and two laser beams (Nd:YAG, 532 nm) successively, where their velocities could be determined. Then a pulsed laser (266 nm) downstream was triggered, on the basis of the velocities, to desorb and/or ionize the particles. The produced positive and negative molecular fragments were recorded.[31] The vacuum aerodynamic diameter of individual particles corresponded to the measured velocities, which were calibrated with standard polystyrene latex spheres (Duke Scientific Corp., Palo Alto, CA) with sizes ranging between 0.22 and 2.0 μm.

Data Analysis. The single-particle size and mass spectral analysis were performed using the FATES toolkit built in MATLAB (The MathWorks, Inc.).[32] Overall, 9 866 142 particles were obtained with both positive and negative spectral information. Most of the particles' aerodynamic diameters ranged from 200 to 700 nm and peaked at 450−550 nm (Figure S2). The hourly mean number fraction (Nf) and relative peak areas (RPA, which represents the percentage contribution of the targeted ion peak area to the sum of all ion peak areas) are applied to indicate the variations of various species in individual particles.

To identify the ion markers for IMs, various standard solutions (Sigma-Aldrich), including 4-methylimidazole (MIM), 2-ethylimidazole (EI), 2,4-dimethylimidazole (DMI), IC, and BM, were atomized and introduced into the SPAMS. Note that these IMs represent the most abundant fraction identified in the atmosphere.[1,2,9] Approximately 50 000

https://doi.org/10.1021/acs.estlett.2c00029
Environ. Sci. Technol. Lett. 2022, 9, 265−271

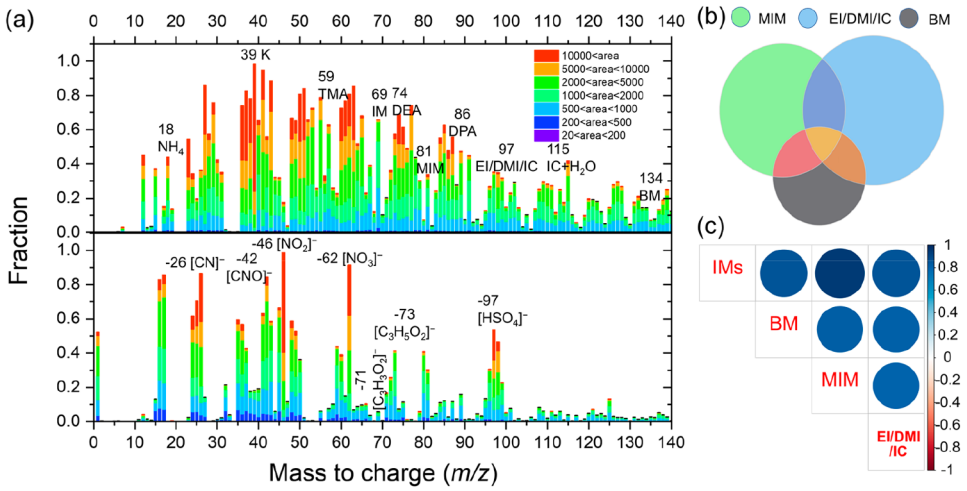

Figure 2. (a) Number fraction of ion peaks in all of the IMs-containing particles. The stacked color map indicates the range of the ion peak area. (b) Venn diagram of the number-based mixing state involving EI, DMI, and IC (green circle), MIM (blue circle), and BM (gray circle). (c) Correlation matrix of hourly detected particle numbers of IMs-containing particles. The colors indicate the correlation coefficient (r).

particles with both positive and negative spectral data were obtained.

As substantially important precursors of IMs,[29] carbonyl-containing particles are distinguished by m/z −71 $[C_3H_3O_2]^-$ (methylglyoxal or acrylate) and m/z −73 $[C_3H_5O_2]^-$ (glyoxylate) that originated from oxidation of glyoxal,[6] ammonium by m/z 18 $[NH_4]^+$, and amines by m/z 59 $[(CH_3)_3N]^+$ (TMA), m/z 74 $[(C_2H_5)_2NH_2]^+$ (DEA), or m/z 86 $[(C_2H_5)_2NCH_2]^+$ (DPA).[33−35] Other related species include formic acid at m/z −45 $[HCO_2]^-$ and organic nitrogen at m/z −26 $[CN]^-$ and m/z −42 $[CNO]^-$.[36]

Multiple linear and random forest analyses are applied to estimate the relative contribution of several factors to the variations in IMs. In the multiple linear models, the least-squares fit is used, and two of the most common measures of the model fit are the residual standard error and the proportion of variance explained (R^2).[37,38] As a nonlinear multiple regression, random forest first creates multiple decision trees, and each tree grows on the basis of the bootstrap resampling method. The relative importance of the predictors can be presented as the "mean decrease accuracy". In addition, the U.S. Environmental Protection Agency's Positive Matrix Factorization 5.0 (PMF)[39] is applied to analyze the possible sources of IMs, based on the hourly averaged RPAs of IMs, their precursors, and marker ions of potential sources, as detailed in Text S3.

RESULTS AND DISCUSSION

Identification of Various IMs and Their Mixing States.

Laboratory tests show that all of the IMs exhibit distinct marker ions at m/z 68 $[C_3H_4N_2]^+$, m/z 69 $[C_3H_4N_2 + H]^+$, m/z 81 $[C_4H_5N_2]^+$, m/z 134 $[C_6H_6N_4]^+$, and m/z 97 $[C_5H_8N_2 + H]^+/[C_4H_4N_2O + H]^+$, as shown in Figure S3. Some of these markers, i.e., m/z 69 for IMs, m/z 97 for IC, and m/z 135 for BM, have also been similarly found in the laboratory by Hamilton et al.,[6] using an aerosol time-of-flight mass spectrometer. Our analysis further indicates the potential interference at m/z 68, the majority of which are most probably assigned to the Zn-containing particles, marked by Zn (m/z 64, 66, and 68) and ZnCl (m/z 99, 101, and 103) (Figure S4). To avoid interference by m/z 81, sea-salt particles (m/z 23 $[Na]^+$, m/z 62 $[Na_2O]^+$, and m/z 81 $[Na_2Cl]^+$) were also excluded. IMs-containing particles are then regarded as those containing m/z 69, 81, 134, and 97.

Overall, ∼950 000 IMs-containing particles were identified, accounting for ∼10% of all of the measured particles. Specifically, MIM-containing particles (480861), EI-, DMI-, and IC-containing particles (383244), and BM-containing particles (208600) account for ∼5%, ∼4%, and ∼2%, respectively (Table S1). The number fraction is higher than those (1.4−2.9%) reported for southern China,[29] which may be attributed to the higher abundance of precursors as discussed below.

Figure 2a illustrates the Nf of each ion peak detected in the IMs-containing particles. It is obvious that m/z 69 represents the dominant ion peak (67%), followed by MIM (34%), EI, DMI, and IC (27%), and BM ion peaks (15%). Approximately 20% of the MIM-containing particles are mixed with EI, DMI, and IC, and 30% of the BM-containing particles are mixed with EI, DMI, and IC. These internally mixed Nfs (>20%) are obviously higher than those (<5%) for all of the detected particles. The ion fragments of IMs, including m/z 28 $[C_2H_4]^+$, m/z 42 $[C_2H_4N]^+$, and m/z 54 $[C_3H_4N]^+$, and organic nitrogen markers (e.g., m/z −26 $[CN]^-$ and m/z −42 $[CNO]^-$), are also enriched in the IMs-containing particles (Figure S5). The enhanced association (>40% by number) of these ion peaks with the IMs-containing particles also suggests their similar origins. In addition, the hourly detected particle numbers of the identified IMs show high correlations [$r > 0.86$; $p < 0.01$ (Figure 2c)], and they are highly internally mixed with each other (Figure 2b). These results also indicate the appropriate assignment of IMs in this study. It should be noted that it is the most probable assignment of IMs because other types of interference from various organics cannot be eliminated through the SPAMS measurements.

One can also see from Figure 2 that IMs are extensively internally mixed with secondary products such as sulfate (59%), nitrate (98%), and precursors like carbonyls (40%) and amine (56%) or ammonium (54%). The detailed mixing states of IMs with their precursors are listed in Table S2. The proportions of MIM, BM, and EI, DMI, and IC in the carbonyl- and ammonium/amine-containing particles (2−5%)

https://doi.org/10.1021/acs.estlett.2c00029
Environ. Sci. Technol. Lett. 2022, 9, 265−271

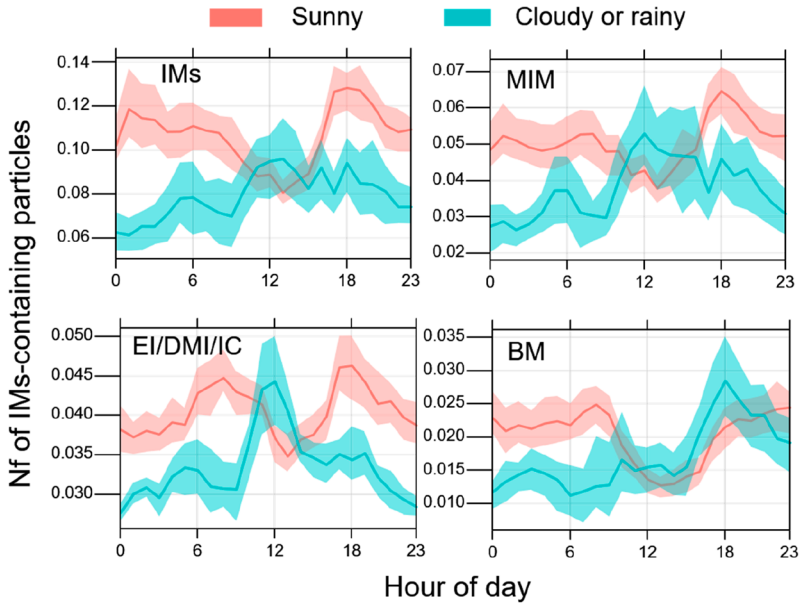

Figure 3. Diurnal variations of the IMs-containing particles during the sunny and cloudy/rainy days. The line and the shaded areas represent the mean and 25−75% values, respectively. There were 10 cloudy or rainy days and 18 sunny days during the observation.

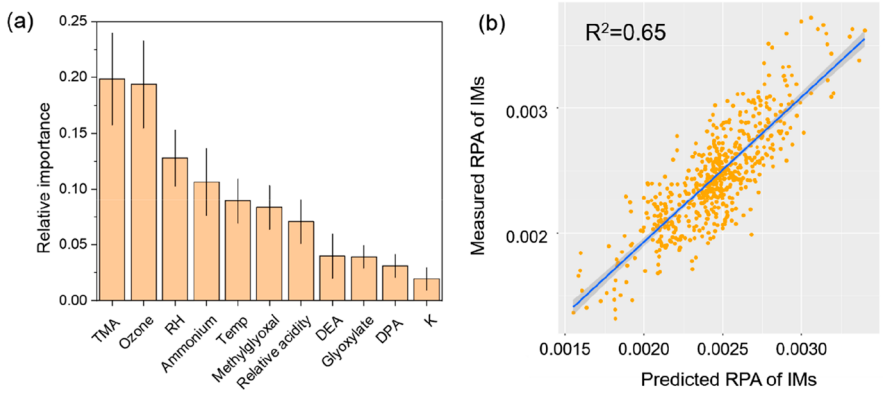

Figure 4. (a) Relative importance of factors for the variation of IMs determined by multilinear regression. The error bars provide 90% confidence intervals with 100 bootstrap replicates to evaluate the results. (b) Relationship between the measured and predicted RPA of IMs.

are obviously higher than those in all detected particles (3−17%). Furthermore, the hourly detected particle number of the IMs-containing particles is also highly correlated with those of their precursors [$r > 0.5$; $p < 0.01$ (Figure S6)]. A similar correlation between MIM and carbonyls such as glyoxal and methylglyoxal has also been reported.[28] These results support the formation pathway of IMs from carbonyls and ammonium/amine, as identified by extensive laboratory studies.[5,19,40,41]

Diurnal Variation of IMs-Containing Particles. The normalized (divided by their mean values) diurnal variations of the mean Nf of the IMs-containing particles are shown in Figure 1d. The diurnal variations of all of the IMs-containing particle types are distinct, decreasing from dawn to noon, with a valley at approximately 13:00 (local time). The peaks of different IMs are slightly different but generally the same at night. The peaks of MIM and EI, DMI, and IC appear around 18:00. The peak of BM appears around midnight, which may be due to the formation of BM from IC reacting with glyoxal and ammonium.[8] The RPAs of IMs and BM also show similar diurnal variation, which is similar to the result of a previous study reporting a higher concentration of IMs at night.[9] The diurnal trend of the IMs-containing particles is similar to those of RH and NO_2 and the reverse of that of temperature and O_3. The results may point to the significant influence of photochemical processes. While carbonyl-based VOCs like glyoxal and methylglyoxal can be directly emitted by vehicles[42,43] and thus contribute to the formation of imidazoles, it is currently believed that vehicle emission accounts for only a small part.[44,45]

First, via comparison of the diurnal variation of the IMs-containing particles on sunny and cloudy days, one can clearly see that the minimum value of IMs in the afternoon of cloudy days is significantly higher than that on sunny days (Figure 3), indicating that stronger sunlight has a critical impact on the diurnal variation of IMs. In contrast, the Nfs of the IMs-containing particles increase from 9:00 to 12:00 during the cloudy/rainy days and peak at 12:00. Second, the RPA of IMs shows a significant negative correlation with O_3 ($r = -0.77$; $p < 0.01$), and the Nf of the IMs-containing particles also decreases with an increase in O_3 (Figure S7). This is most probably due to degradation of IMs by photochemistry processes, most probably through the oxidation by O_3 and

https://doi.org/10.1021/acs.estlett.2c00029
Environ. Sci. Technol. Lett. 2022, 9, 265−271

OH radicals.[24,25] Finally, to verify the photochemical reactions of IMs, we simulated the direct photolysis and photochemistry reactions of different IMs in the laboratory (as detailed in Text S2). All of the IMs show significant degradation under sunlight or simulated UV light (254 nm), and the reaction rate is 1 order of magnitude faster after the addition of OH radicals upon introduction of H_2O_2 (Figure S8).

Controlling Factors of IMs in Ambient Aerosol. Multiple linear regression and random forest analysis are further applied to quantitatively estimate the relative contribution of the potentially influential factors, namely, temperature, RH, O_3, relative acidity, RPA of potassium (K, m/z 39), and precursors such as ammonium, amines, and carbonyls. Potassium tracks the intensity of biomass burning, whereas temperature and O_3 track the strength of photochemistry.[46] RH may affect the gas-to-particle partitioning of both ammonia/amine- and carbonyl-based precursors,[47,48] and the relative number of deliquesced aqueous aerosols,[49] which changes both the internal mixing and chemistry of aerosols and the gas−aerosol partitioning of precursors, thus affecting the formation of IMs. The relative acidity of aerosol particles, herein defined as the peak area ratio (i.e., sulfate and nitrate divided by ammonium),[50] may affect the reaction rates and pathways for the formation of IMs.[7]

As shown in Figure 4, the variations of IMs can be explained well (R^2 = 0.65; p < 0.01) by these input factors, with the evaluation of the model performance provided in Figure S9. The estimated importance of each factor shows that imidazole chemistry is mainly dependent on precursors (ammonium, amines, and carbonyls; 50%), the strength of photochemistry (temperature and O_3, 28%), and RH (13%). The limited contribution (<5%) from the K factor indicates a negligible influence of biomass burning. Similarly, random forest analysis can predict ∼63% of the variations of IMs, and the three most important predictors are precursors, the strength of photochemistry, and RH. Consistently, the importance of various precursors can also be supported by the PMF results, which shows that amines, ammonium, and carbonyl compound factors together explain ∼50% of the observed IMs (Text S3 and Figure S10). To further confirm the importance of photochemical reactions, we compare the relative importance of each factor for the sunny and cloudy/rainy days, on the basis of random forest analysis. The results show that O_3 (24%) is the most crucial meteorological factor for the sunny days, whereas it is the least important factor (8%) for the cloudy/rainy days (Figure S11). One can also see that RH likely plays a more important role than ozone on cloudy days, which is in contrast with that for sunny days. We may conclude that the variation of imidazole compounds is mainly affected by photochemistry on sunny days but by the precursors and relative humidity on cloudy days. It should be noted that our conclusions based on a relatively narrow time period may not be universal for other seasons with distinctly different meteorological conditions. However, the controlling factors for the atmospheric processing of IMs in ambient aerosol may still be indicative.

■ ASSOCIATED CONTENT

Supporting Information

The Supporting Information is available free of charge at https://pubs.acs.org/doi/10.1021/acs.estlett.2c00029.

Additional experimental details and results, including 11 figures and three tables (PDF)

■ AUTHOR INFORMATION

Corresponding Author

Guohua Zhang − *State Key Laboratory of Organic Geochemistry and Guangdong Key Laboratory of Environmental Protection and Resources Utilization, Guangzhou Institute of Geochemistry, Chinese Academy of Sciences (CAS), Guangzhou 510640, P. R. China; CAS Center for Excellence in Deep Earth Science, Guangzhou 510640, P. R. China; Guangdong-Hong Kong-Macao Joint Laboratory for Environmental Pollution and Control, Guangzhou 510640, P. R. China;* orcid.org/0000-0002-6153-0748; Email: zhanggh@gig.ac.cn

Authors

Xiaodong Hu − *State Key Laboratory of Organic Geochemistry and Guangdong Key Laboratory of Environmental Protection and Resources Utilization, Guangzhou Institute of Geochemistry, Chinese Academy of Sciences (CAS), Guangzhou 510640, P. R. China; CAS Center for Excellence in Deep Earth Science, Guangzhou 510640, P. R. China; University of Chinese Academy of Sciences, Beijing 100049, P. R. China*

Ziyong Guo − *State Key Laboratory of Organic Geochemistry and Guangdong Key Laboratory of Environmental Protection and Resources Utilization, Guangzhou Institute of Geochemistry, Chinese Academy of Sciences (CAS), Guangzhou 510640, P. R. China; CAS Center for Excellence in Deep Earth Science, Guangzhou 510640, P. R. China; University of Chinese Academy of Sciences, Beijing 100049, P. R. China*

Wei Sun − *State Key Laboratory of Organic Geochemistry and Guangdong Key Laboratory of Environmental Protection and Resources Utilization, Guangzhou Institute of Geochemistry, Chinese Academy of Sciences (CAS), Guangzhou 510640, P. R. China; CAS Center for Excellence in Deep Earth Science, Guangzhou 510640, P. R. China; University of Chinese Academy of Sciences, Beijing 100049, P. R. China*

Xiufeng Lian − *State Key Laboratory of Organic Geochemistry and Guangdong Key Laboratory of Environmental Protection and Resources Utilization, Guangzhou Institute of Geochemistry, Chinese Academy of Sciences (CAS), Guangzhou 510640, P. R. China; CAS Center for Excellence in Deep Earth Science, Guangzhou 510640, P. R. China; University of Chinese Academy of Sciences, Beijing 100049, P. R. China;* Present Address: X.L.: Institute of Mass Spectrometer and Atmospheric Environment, Jinan University, Guangzhou 510632, P. R. China

Yuzhen Fu − *State Key Laboratory of Organic Geochemistry and Guangdong Key Laboratory of Environmental Protection and Resources Utilization, Guangzhou Institute of Geochemistry, Chinese Academy of Sciences (CAS), Guangzhou 510640, P. R. China; CAS Center for Excellence in Deep Earth Science, Guangzhou 510640, P. R. China; University of Chinese Academy of Sciences, Beijing 100049, P. R. China*

He Meng − *Qingdao Eco-environment Monitoring Center of Shandong Province, Qingdao 266003, P. R. China*

Yujiao Zhu − *Environment Research Institute, Shandong University, Qingdao 266237, P. R. China*

https://doi.org/10.1021/acs.estlett.2c00029
Environ. Sci. Technol. Lett. 2022, 9, 265−271

Xinfeng Wang − *Environment Research Institute, Shandong University, Qingdao 266237, P. R. China;* orcid.org/0000-0003-0911-7312

Likun Xue − *Environment Research Institute, Shandong University, Qingdao 266237, P. R. China;* orcid.org/0000-0001-7329-2110

Xinhui Bi − *State Key Laboratory of Organic Geochemistry and Guangdong Key Laboratory of Environmental Protection and Resources Utilization, Guangzhou Institute of Geochemistry, Chinese Academy of Sciences (CAS), Guangzhou 510640, P. R. China; CAS Center for Excellence in Deep Earth Science, Guangzhou 510640, P. R. China; Guangdong-Hong Kong-Macao Joint Laboratory for Environmental Pollution and Control, Guangzhou 510640, P. R. China*

Xinming Wang − *State Key Laboratory of Organic Geochemistry and Guangdong Key Laboratory of Environmental Protection and Resources Utilization, Guangzhou Institute of Geochemistry, Chinese Academy of Sciences (CAS), Guangzhou 510640, P. R. China; CAS Center for Excellence in Deep Earth Science, Guangzhou 510640, P. R. China; Guangdong-Hong Kong-Macao Joint Laboratory for Environmental Pollution and Control, Guangzhou 510640, P. R. China;* orcid.org/0000-0002-1982-0928

Ping'an Peng − *State Key Laboratory of Organic Geochemistry and Guangdong Key Laboratory of Environmental Protection and Resources Utilization, Guangzhou Institute of Geochemistry, Chinese Academy of Sciences (CAS), Guangzhou 510640, P. R. China; CAS Center for Excellence in Deep Earth Science, Guangzhou 510640, P. R. China; Guangdong-Hong Kong-Macao Joint Laboratory for Environmental Pollution and Control, Guangzhou 510640, P. R. China*

Complete contact information is available at: https://pubs.acs.org/10.1021/acs.estlett.2c00029

Notes

The authors declare no competing financial interest.

■ ACKNOWLEDGMENTS

This work was funded by the Natural Science Foundation of Guangdong Province (2019B151502022), the National Natural Science Foundation of China (42077322, 41775124, and 41877307), the Youth Innovation Promotion Association CAS (2021354), and the Guangdong Foundation for Program of Science and Technology Research (2019B121205006 and 2020B1212060053). The authors are also grateful for the assistance of Lei Li and Xubing Du in the maintenance of the SPAMS instrument. This is contribution No.IS-3158 from GIGCAS.

■ REFERENCES

(1) Gao, K.; Zhang, Y.; Liu, Y.; Yang, M.; Zhu, T. Screening of Imidazoles in Atmospheric Aerosol Particles Using a Hybrid Targeted and Untargeted Method Based on Ultra-Performance Liquid Chromatography-Quadrupole Time-of-Flight Mass Spectrometry. *Anal. Chim. Acta* **2021**, *1163*, 338516.

(2) Takao, Y.; Atarashi, T.; Kubo, T.; Nagae, M.; Nakayama, T. Quantification of Imidazole Compounds in Ambient Aerosols at Suburban and Forest Sites in Western Japan. *Asian J. Atmos. Environ.* **2019**, *13* (4), 259−265.

(3) Tinel, L.; Dumas, S.; George, C. A Time-Resolved Study of the Multiphase Chemistry of Excited Carbonyls: Imidazole-2-Carboxaldehyde and Halides. *Comptes Rendus Chim.* **2014**, *17* (7−8), 801−807.

(4) Aregahegn, K. Z.; Nozière, B.; George, C. Organic Aerosol Formation Photo-Enhanced by the Formation of Secondary Photosensitizers in Aerosols. *Faraday Discuss.* **2013**, *165*, 123−134.

(5) Yu, G.; Bayer, A. R.; Galloway, M. M.; Korshavn, K. J.; Fry, C. G.; Keutsch, F. N. Glyoxal in Aqueous Ammonium Sulfate Solutions: Products, Kinetics and Hydration Effects. *Environ. Sci. Technol.* **2011**, *45* (15), 6336−6342.

(6) Hamilton, J. F.; Baeza-Romero, M. T.; Finessi, E.; Rickard, A. R.; Healy, R. M.; Peppe, S.; Adams, T. J.; Daniels, M. J. S.; Ball, S. M.; Goodall, I. C. A.; Monks, P. S.; Borrás, E.; Muñoz, A. Online and Offline Mass Spectrometric Study of the Impact of Oxidation and Ageing on Glyoxal Chemistry and Uptake onto Ammonium Sulfate Aerosols. *Faraday Discuss.* **2013**, *165*, 447−472.

(7) Sedehi, N.; Takano, H.; Blasic, V. A.; Sullivan, K. A.; De Haan, D. O. Temperature- and PH-Dependent Aqueous-Phase Kinetics of the Reactions of Glyoxal and Methylglyoxal with Atmospheric Amines and Ammonium Sulfate. *Atmos. Environ.* **2013**, *77*, 656−663.

(8) Kampf, C. J.; Jakob, R.; Hoffmann, T. Identification and Characterization of Aging Products in the Glyoxal/Ammonium Sulfate System — Implications for Light-Absorbing Material in Atmospheric Aerosols. *Atmos. Chem. Phys.* **2012**, *12* (14), 6323−6333.

(9) Teich, M.; Van Pinxteren, D.; Kecorius, S.; Wang, Z.; Herrmann, H. First Quantification of Imidazoles in Ambient Aerosol Particles: Potential Photosensitizers, Brown Carbon Constituents, and Hazardous Components. *Environ. Sci. Technol.* **2016**, *50* (3), 1166−1173.

(10) Laskin, A.; Smith, J. S.; Laskin, J. Molecular Characterization of Nitrogen-Containing Organic Compounds in Biomass Burning Aerosols Using High-Resolution Mass Spectrometry. *Environ. Sci. Technol.* **2009**, *43* (10), 3764−3771.

(11) Teich, M.; Schmidtpott, M.; van Pinxteren, D.; Chen, J.; Herrmann, H. Separation and Quantification of Imidazoles in Atmospheric Particles Using LC-Orbitrap-MS. *J. Sep. Sci.* **2020**, *43* (3), 577−589.

(12) Nozière, B.; Dziedzic, P.; Córdova, A. Products and Kinetics of the Liquid-Phase Reaction of Glyoxal Catalyzed by Ammonium Ions (NH_4^+). *J. Phys. Chem. A* **2009**, *113* (1), 231−237.

(13) Kirkland, J. R.; Lim, Y. B.; Tan, Y.; Altieri, K. E.; Turpin, B. J. Glyoxal Secondary Organic Aerosol Chemistry: Effects of Dilute Nitrate and Ammonium and Support for Organic Radical-Radical Oligomer Formation. *Environ. Chem.* **2013**, *10* (3), 158−166.

(14) Galloway, M. M.; Loza, C. L.; Chhabra, P. S.; Chan, A. W. H.; Yee, L. D.; Seinfeld, J. H.; Keutsch, F. N. Analysis of Photochemical and Dark Glyoxal Uptake: Implications for SOA Formation. *Geophys. Res. Lett.* **2011**, *38*, L17811.

(15) De Haan, D. O.; Corrigan, A. L.; Smith, K. W.; Stroik, D. R.; Turley, J. J.; Lee, F. E.; Tolbert, M. A.; Jimenez, J. L.; Cordova, K. E.; Ferrell, G. R. Secondary Organic Aerosol-Forming Reactions of Glyoxal with Amino Acids. *Environ. Sci. Technol.* **2009**, *43* (8), 2818−2824.

(16) De Haan, D. O. Aqueous Aerosol Processing of Glyoxal and Methylglyoxal: Recent Measurements of Uptake Coefficients, SOA Production, and Brown Carbon Formation. *ACS Symp. Ser.* **2018**, *1299*, 149−167.

(17) Ortiz-Montalvo, D. L.; Häkkinen, S. A. K.; Schwier, A. N.; Lim, Y. B.; McNeill, V. F.; Turpin, B. J. Ammonium Addition (and Aerosol PH) Has a Dramatic Impact on the Volatility and Yield of Glyoxal Secondary Organic Aerosol. *Environ. Sci. Technol.* **2014**, *48* (1), 255−262.

(18) Jang, M.; Czoschke, N. M.; Northcross, A. L.; Cao, G.; Shaof, D. SOA Formation from Partitioning and Heterogeneous Reactions: Model Study in the Presence of Inorganic Species. *Environ. Sci. Technol.* **2006**, *40*, 3013−3022.

(19) Galloway, M. M.; Chhabra, P. S.; Chan, A. W. H.; Surratt, J. D.; Flagan, R. C.; Seinfeld, J. H.; Keutsch, F. N. Glyoxal Uptake on

Ammonium Sulphate Seed Aerosol: Reaction Products and Reversibility of Uptake under Dark and Irradiated Conditions. *Atmos. Chem. Phys.* **2009**, *9* (10), 3331−3345.
(20) Grace, D. N.; Sharp, J. R.; Holappa, R. E.; Lugos, E. N.; Sebold, M. B.; Griffith, D. R.; Hendrickson, H. P.; Galloway, M. M. Heterocyclic Product Formation in Aqueous Brown Carbon Systems. *ACS Earth Sp. Chem.* **2019**, *3*, 2472−2481.
(21) De Haan, D. O.; Hawkins, L. N.; Welsh, H. G.; Pednekar, R.; Casar, J. R.; Pennington, E. A.; De Loera, A.; Jimenez, N. G.; Symons, M. A.; Zauscher, M.; Pajunoja, A.; Caponi, L.; Cazaunau, M.; Formenti, P.; Gratien, A.; Pangui, E.; Doussin, J. F. Brown Carbon Production in Ammonium- or Amine-Containing Aerosol Particles by Reactive Uptake of Methylglyoxal and Photolytic Cloud Cycling. *Environ. Sci. Technol.* **2017**, *51* (13), 7458−7466.
(22) Marrero-Ortiz, W.; Hu, M.; Du, Z.; Ji, Y.; Wang, Y. Y.; Guo, S.; Lin, Y.; Gomez-Hermandez, M.; Peng, J.; Li, Y.; Secrest, J.; Zamora, M. L.; Wang, Y. Y.; An, T.; Zhang, R. Formation and Optical Properties of Brown Carbon from Small α-Dicarbonyls and Amines. *Environ. Sci. Technol.* **2019**, *53* (1), 117−126.
(23) Kasthuriarachchi, N. Y.; Rivellini, L. H.; Chen, X.; Li, Y. J.; Lee, A. K. Y. Effect of Relative Humidity on Secondary Brown Carbon Formation in Aqueous Droplets. *Environ. Sci. Technol.* **2020**, *54* (20), 13207−13216.
(24) Felber, T.; Schaefer, T.; Herrmann, H. OH-Initiated Oxidation of Imidazoles in Tropospheric Aqueous-Phase Chemistry. *J. Phys. Chem. A* **2019**, *123* (8), 1505−1513.
(25) Tekle-Röttering, A.; Lim, S.; Reisz, E.; Lutze, H. V.; Abdighahroudi, M. S.; Willach, S.; Schmidt, W.; Tentscher, P. R.; Rentsch, D.; Mcardell, C. S.; Schmidt, T. C.; von Gunten, U. Reactions of pyrrole, imidazole, and pyrazole with ozone: kinetics and mechanisms. *Environ. Sci.: Water Res. Technol.* **2020**, *6*, 976−992.
(26) Pryor, W. A.; Giamalva, D. H.; Church, D. F. Kinetics of Ozonation. 2. Amino Acids and Model Compounds in Water and Comparisons to Rates in Nonpolar Solvents. *J. Am. Chem. Soc.* **1984**, *106*, 7094−7100.
(27) Sharp, J. R.; Grace, D. N.; Ma, S.; Woo, J. L.; Galloway, M. M. Competing Photochemical Effects in Aqueous Carbonyl/Ammonium Brown Carbon Systems. *ACS Earth Sp. Chem.* **2021**, *5*, 1902−1915.
(28) He, C.; Wang, H.; Gong, D.; Lv, S.; Wu, G.; Wang, R.; Chen, Y.; Ding, Y.; Li, Y.; Wang, B. Insights into High Concentrations of Particle-Bound Imidazoles in the Background Atmosphere of Southern China: Potential Sources and Influencing Factors. *Sci. Total Environ.* **2022**, *806*, 150804.
(29) Lian, X.; Zhang, G.; Yang, Y.; Lin, Q.; Fu, Y.; Jiang, F.; Peng, L.; Hu, X.; Chen, D.; Wang, X.; Peng, P.; Sheng, G.; Bi, X. Evidence for the Formation of Imidazole from Carbonyls and Reduced Nitrogen Species at the Individual Particle Level in the Ambient Atmosphere. *Environ. Sci. Technol. Lett.* **2021**, *8* (1), 9−15.
(30) Cui, S.; Xian, J.; Shen, F.; Zhang, L.; Deng, B.; Zhang, Y.; Ge, X. One-Year Real-Time Measurement of Black Carbon in the Rural Area of Qingdao, Northeastern China: Seasonal Variations, Meteorological Effects, and the Covid-19 Case Analysis. *Atmosphere* **2021**, *12* (3), 394.
(31) Li, L.; Huang, Z.; Dong, J.; Li, M.; Gao, W.; Nian, H.; Fu, Z.; Zhang, G.; Bi, X.; Cheng, P.; Zhou, Z. Real Time Bipolar Time-of-Flight Mass Spectrometer for Analyzing Single Aerosol Particles. *Int. J. Mass Spectrom.* **2011**, *303* (2−3), 118−124.
(32) Sultana, C. M.; Cornwell, G. C.; Rodriguez, P.; Prather, K. A. FATES: A Flexible Analysis Toolkit for the Exploration of Single-Particle Mass Spectrometer Data. *Atmos. Meas. Technol.* **2017**, *10* (4), 1323−1334.
(33) Cheng, C.; Huang, Z.; Chan, C. K.; Chu, Y.; Li, M.; Zhang, T.; Ou, Y.; Chen, D.; Cheng, P.; Li, L.; Gao, W.; Huang, Z.; Huang, B.; Fu, Z.; Zhou, Z. Characteristics and Mixing State of Amine-Containing Particles at a Rural Site in the Pearl River Delta, China. *Atmos. Chem. Phys.* **2018**, *18* (12), 9147−9159.
(34) Zhang, G.; Bi, X.; Li, L.; Chan, L. Y.; Li, M.; Wang, X.; Sheng, G.; Fu, J.; Zhou, Z. Mixing State of Individual Submicron Carbon-Containing Particles during Spring and Fall Seasons in Urban Guangzhou, China: A Case Study. *Atmos. Chem. Phys.* **2013**, *13*, 4723−4735.
(35) Li, Z.; Zhou, R.; Wang, Y.; Wang, G.; Chen, M.; Li, Y.; Wang, Y.; Yi, Y.; Hou, Z.; Guo, Q.; Meng, J. Characteristics and Sources of Amine-Containing Particles in the Urban Atmosphere of Liaocheng, a Seriously Polluted City in North China during the COVID-19 Outbreak. *Environ. Pollut.* **2021**, *289* (May), 117887.
(36) Zawadowicz, M. A.; Froyd, K. D.; Murphy, D. M.; Cziczo, D. J. Improved Identification of Primary Biological Aerosol Particles Using Single-Particle Mass Spectrometry. *Atmos. Chem. Phys.* **2017**, *17* (11), 7193−7212.
(37) Czoschke, N. M.; Jang, M. Acidity Effects on the Formation of α-Pinene Ozone SOA in the Presence of Inorganic Seed. *Atmos. Environ.* **2006**, *40* (23), 4370−4380.
(38) Yu, Q.; Chen, J.; Qin, W.; Cheng, S.; Zhang, Y.; Ahmad, M.; Ouyang, W. Characteristics and Secondary Formation of Water-Soluble Organic Acids in PM 1, PM 2.5 and PM 10 in Beijing during Haze Episodes. *Sci. Total Environ.* **2019**, *669*, 175−184.
(39) Giorio, C.; Tapparo, A.; Dall'Osto, M.; Beddows, D. C. S.; Esser-Gietl, J. K.; Healy, R. M.; Harrison, R. M. Local and Regional Components of Aerosol in a Heavily Trafficked Street Canyon in Central London Derived from PMF and Cluster Analysis of Single-Particle ATOFMS Spectra. *Environ. Sci. Technol.* **2015**, *49* (6), 3330−3340.
(40) Kua, J.; Krizner, H. E.; De Haan, D. O. Thermodynamics and Kinetics of Imidazole Formation from Glyoxal, Methylamine, and Formaldehyde: A Computational Study. *J. Phys. Chem. A* **2011**, *115* (9), 1667−1675.
(41) Rodriguez, A. A.; De Loera, A.; Powelson, M. H.; Galloway, M. M.; De Haan, D. O. Formaldehyde and Acetaldehyde Increase Aqueous-Phase Production of Imidazoles in Methylglyoxal/Amine Mixtures: Quantifying a Secondary Organic Aerosol Formation Mechanism. *Environ. Sci. Technol. Lett.* **2017**, *4* (6), 234−239.
(42) Zhang, Y.; Wang, X.; Wen, S.; Herrmann, H.; Yang, W.; Huang, X.; Zhang, Z.; Huang, Z.; He, Q.; George, C. On-Road Vehicle Emissions of Glyoxal and Methylglyoxal from Tunnel Tests in Urban Guangzhou, China. *Atmos. Environ.* **2016**, *127*, 55−60.
(43) Wu, Z.; Zhang, Y.; Pei, C.; Huang, Z.; Wang, Y.; Chen, Y.; Yan, J.; Huang, X.; Xiao, S.; Luo, S.; Zeng, J.; Wang, J.; Fang, H.; Zhang, R.; Li, S.; Fu, X.; Song, W.; Wang, X. Real-World Emissions of Carbonyls from Vehicles in an Urban Tunnel in South China. *Atmos. Environ.* **2021**, *258*, 118491.
(44) Chen, W. T.; Shao, M.; Lu, S. H.; Wang, M.; Zeng, L. M.; Yuan, B.; Liu, Y. Understanding Primary and Secondary Sources of Ambient Carbonyl Compounds in Beijing Using the PMF Model. *Atmos. Chem. Phys.* **2014**, *14*, 3047−3062.
(45) Lui, K. H.; Dai, W. T.; Chan, C. S.; Ho, S. S. H.; Cao, J. J.; Lee, S. C.; Ho, K. F. Spatial Distributions of Airborne Di-Carbonyls in Urban and Rural Areas in China. *Atmos. Res.* **2017**, *186*, 1−8.
(46) He, L. Y.; Huang, X. F.; Xue, L.; Hu, M.; Lin, Y.; Zheng, J.; Zhang, R.; Zhang, Y. H. Submicron Aerosol Analysis and Organic Source Apportionment in an Urban Atmosphere in Pearl River Delta of China Using High-Resolution Aerosol Mass Spectrometry. *J. Geophys. Res.: Atmos.* **2011**, *116*, D12.
(47) Ge, X.; Wexler, A. S.; Clegg, S. L. Atmospheric Amines - Part I. A Review. *Atmos. Environ.* **2011**, *45* (3), 524−546.
(48) Rao, G.; Vejerano, E. P. Partitioning of Volatile Organic Compounds to Aerosols: A Review. *Chemosphere* **2018**, *212*, 282−296.
(49) Ge, Z.; Wexler, A. S.; Johnston, M. V. Deliquescence Behavior of Multicomponent Aerosols. *J. Phys. Chem. A* **1998**, *102* (1), 173−180.
(50) Pratt, K. A.; Hatch, L. E.; Prather, K. A. Seasonal Volatility Dependence of Ambient Particle Phase Amines. *Environ. Sci. Technol.* **2009**, *43* (14), 5276−5281.

https://doi.org/10.1021/acs.estlett.2c00029
Environ. Sci. Technol. Lett. 2022, 9, 265−271